

## Accepted Manuscript

Reevaluation of Fenpropimorph as a  $\sigma$  Receptor Ligand: Structure-Affinity Relationship Studies at Human  $\sigma_1$  Receptors

Elena Sguazzini, Hayden R. Schmidt, Kavita A. Iyer, Andrew C. Kruse, Małgorzata Dukat

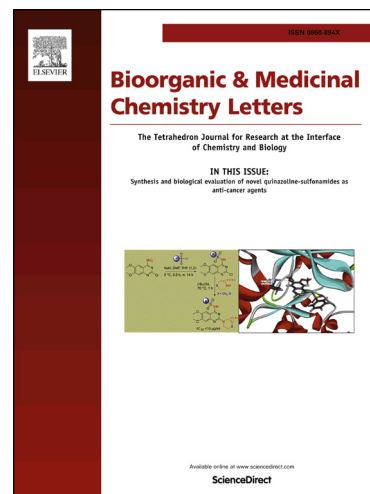
PII: S0960-894X(17)30474-2  
DOI: <http://dx.doi.org/10.1016/j.bmcl.2017.04.088>  
Reference: BMCL 24941

To appear in: *Bioorganic & Medicinal Chemistry Letters*

Received Date: 10 April 2017  
Accepted Date: 27 April 2017

Please cite this article as: Sguazzini, E., Schmidt, H.R., Iyer, K.A., Kruse, A.C., Dukat, M., Reevaluation of Fenpropimorph as a  $\sigma$  Receptor Ligand: Structure-Affinity Relationship Studies at Human  $\sigma_1$  Receptors, *Bioorganic & Medicinal Chemistry Letters* (2017), doi: <http://dx.doi.org/10.1016/j.bmcl.2017.04.088>

This is a PDF file of an unedited manuscript that has been accepted for publication. As a service to our customers we are providing this early version of the manuscript. The manuscript will undergo copyediting, typesetting, and review of the resulting proof before it is published in its final form. Please note that during the production process errors may be discovered which could affect the content, and all legal disclaimers that apply to the journal pertain.



**Reevaluation of Fenpropimorph as a  $\sigma$  Receptor Ligand: Structure-Affinity  
Relationship Studies at Human  $\sigma_1$  Receptors**

Elena Sguazzini,<sup>a</sup> Hayden R. Schmidt,<sup>b</sup> Kavita A. Iyer,<sup>a</sup> Andrew C. Kruse,<sup>b</sup> Małgorzata  
Dukat<sup>a\*</sup>

<sup>a</sup>*Department of Medicinal Chemistry, Virginia Commonwealth University, Richmond,  
Virginia 23298, USA,*

<sup>b</sup>*Department of Biological Chemistry and Molecular Pharmacology, Harvard Medical  
School, Boston, Massachusetts 02115, USA.*

\*Corresponding author. Tel.: 8048285256; fax: 8048287625.

E-mail address: [mdukat@vcu.edu](mailto:mdukat@vcu.edu) (M. Dukat)

Address: Department of Medicinal Chemistry, School of Pharmacy, Virginia Commonwealth  
University, PO Box 980540, Richmond, VA 23298-540, USA

*Bioorg. Med. Chem. Lett.*\_submitted April 10, 2017

## ABSTRACT

Fenpropimorph (**1**) is considered a “super high-affinity”  $\sigma_1$  receptor ligand ( $K_i = 0.005$  nM for guinea pig  $\sigma_1$  receptors). Here, we examine the binding of **1** and several of its deconstructed analogs at human  $\sigma_1$  ( $h\sigma_1$ ) receptors. We monitored their subtype selectivity by determining the binding affinity at  $\sigma_2$  receptors. In addition, we validated an existing pharmacophore model at the molecular level by conducting 3D molecular modeling studies, using the crystal structure of  $h\sigma_1$  receptors, and Hydrophatic INTeractions (HINT) analysis. Our structure affinity relationship studies showed that **1** binds with lower affinity at  $h\sigma_1$  receptors ( $K_i = 17.3$  nM) compared to guinea pig; moreover, we found that none of the fenpropimorph methyl groups is important for its binding at  $h\sigma_1$  receptors, nor is stereochemistry. For example, removal of all methyl groups as seen in **4** resulted in an almost 5-fold higher affinity at  $h\sigma_1$  receptors compared to **1** and 350-fold selectivity versus  $\sigma_2$  receptors. In addition, although the O atom of the morpholine ring does not contribute to affinity at  $h\sigma_1$  receptors (and might even detract from it), it plays role in subtype ( $\sigma_1$  versus  $\sigma_2$  receptor) selectivity.

## KEY WORDS

SAFiR, Radioligand binding, 3D Molecular modeling, HINT analysis

**1. Introduction**

The sigma1 ( $\sigma_1$ ) receptor<sup>1</sup> experienced a resurgence in interest beginning in 2011 when a familial mutation in the receptor was shown to cause amyotrophic lateral sclerosis (ALS).<sup>2</sup> Since then, the  $\sigma_1$  receptor has emerged as a potential therapeutic target for a variety of neurological disorders including pain, Parkinson's, Alzheimer's and Huntington's diseases, depression, amnesia, and schizophrenia.<sup>3,4</sup>

Originally,  $\sigma$  receptors were classified as a subtype of the opioid receptor superfamily based on radioligand-binding studies,<sup>5</sup> but further pharmacological studies and the molecular cloning of the  $\sigma_1$  receptor confirmed that both it and the pharmacologically similar but genetically distinct  $\sigma_2$  receptor are unrelated to opioid receptors.<sup>6</sup> The  $\sigma_1$  receptor has a particularly diverse pharmacological profile as it can bind a remarkable variety of small molecules with high (<100 nM) affinity. This spurred the creation and identification of a myriad of molecules that can target the receptor. Combined with its emerging disease relevance, the pharmacological tractability of the  $\sigma_1$  receptor makes it an ideal target for therapeutic intervention.

Recently, the Kruse laboratory reported the 3D crystal structure of the human  $\sigma_1$  ( $h\sigma_1$ ) receptor in complex with two structurally and functionally diverse ligands, an antagonist, PD144418 (Figure 1), and the yet to be defined agonist/inverse agonist, *N*-(1-benzylpiperidin-4-yl)-4-iodobenzamide (4-IBP), revealing a trimeric structure with a single transmembrane domain for each protomer.<sup>7</sup>

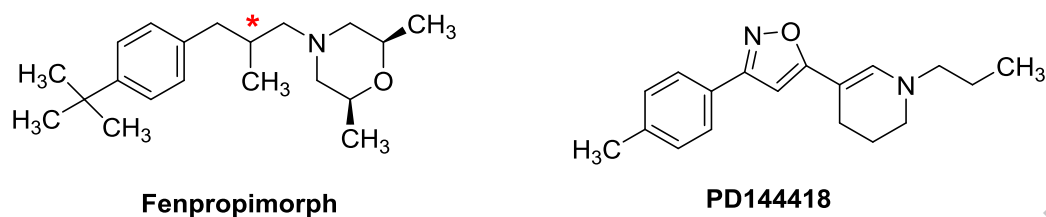


**Figure 1.** Structures of the  $\sigma$  receptor ligands fenpropimorph (**1**) and PD144418.

Fenpropimorph (**1**) is, perhaps, the highest-affinity  $\sigma_1$  receptor ligand ever reported. It binds with extremely high affinity at guinea pig whole-brain ( $K_i = 0.005$  nM) and liver ( $K_i = 0.011$  nM), and yeast-expressed ( $K_i = 0.08$  nM) homogenate  $\sigma_1$  receptors labeled by (+)-[ $^3\text{H}$ ]-pentazocine (PTZ) as radioligand.<sup>8,9</sup> It might be considered as a “super high-affinity”  $\sigma_1$  receptor ligand. Not surprisingly, the Ruoho laboratory used this agent as a scaffold to develop newer, high-affinity  $\sigma_1$  receptor ligands.<sup>10</sup> Unfortunately, it is not known if any of the modifications introduced to the fenpropimorph structure resulted in a higher-affinity ligand than the parent compound because **1** was not used as a positive control in their guinea-pig liver assay.<sup>10</sup>

The picomolar affinity of fenpropimorph makes it a very attractive starting point for the development of novel  $\sigma_1$  receptor agents. But, the question arises: what structural features make fenpropimorph such a high-affinity ligand? Moreover, does fenpropimorph retain comparable picomolar affinity at human  $\sigma_1$  receptors? Here we address these questions, leveraging both synthetic medicinal chemistry, the  $h\sigma_1$  receptor crystal structure, and homology modeling studies, to provide a complete structural analysis of fenpropimorph binding.

We began by examining the binding of fenpropimorph at  $h\sigma_1$  receptors. As an indication of selectivity, we also examined  $\sigma_2$  receptor binding. To understand which structural aspects

of fenpropimorph account for binding to human  $\sigma_1$  receptors we used the “deconstruction-elaboration” approach.<sup>11</sup>

Chemical entities with similar structure had already been synthesized by Glennon’s group,<sup>11</sup> and a  $\sigma_1$  receptor pharmacophore has been proposed.<sup>4,11</sup> Here, we synthesized a new series of fenpropimorph-related compounds to determine if they fit the pharmacophore model and, especially, the recently crystalized structure of the h $\sigma_1$  receptor.<sup>4,7,11</sup> That is, the proposed pharmacophore model suggested that the branched chain between the phenyl ring and amine moiety was not required and that the morpholine oxygen atom should, if anything, slightly detract from binding. The pharmacophore model also implicated a “primary hydrophobic site” at a certain distance from the amine.<sup>4,11</sup> Hence, the hydrophobic *tert*-butyl group of **1** should be a contributor to binding. We prepared a series of analogs to test these hypotheses that we present here in one of the first structure-guided analyses of h $\sigma_1$  receptor pharmacology.

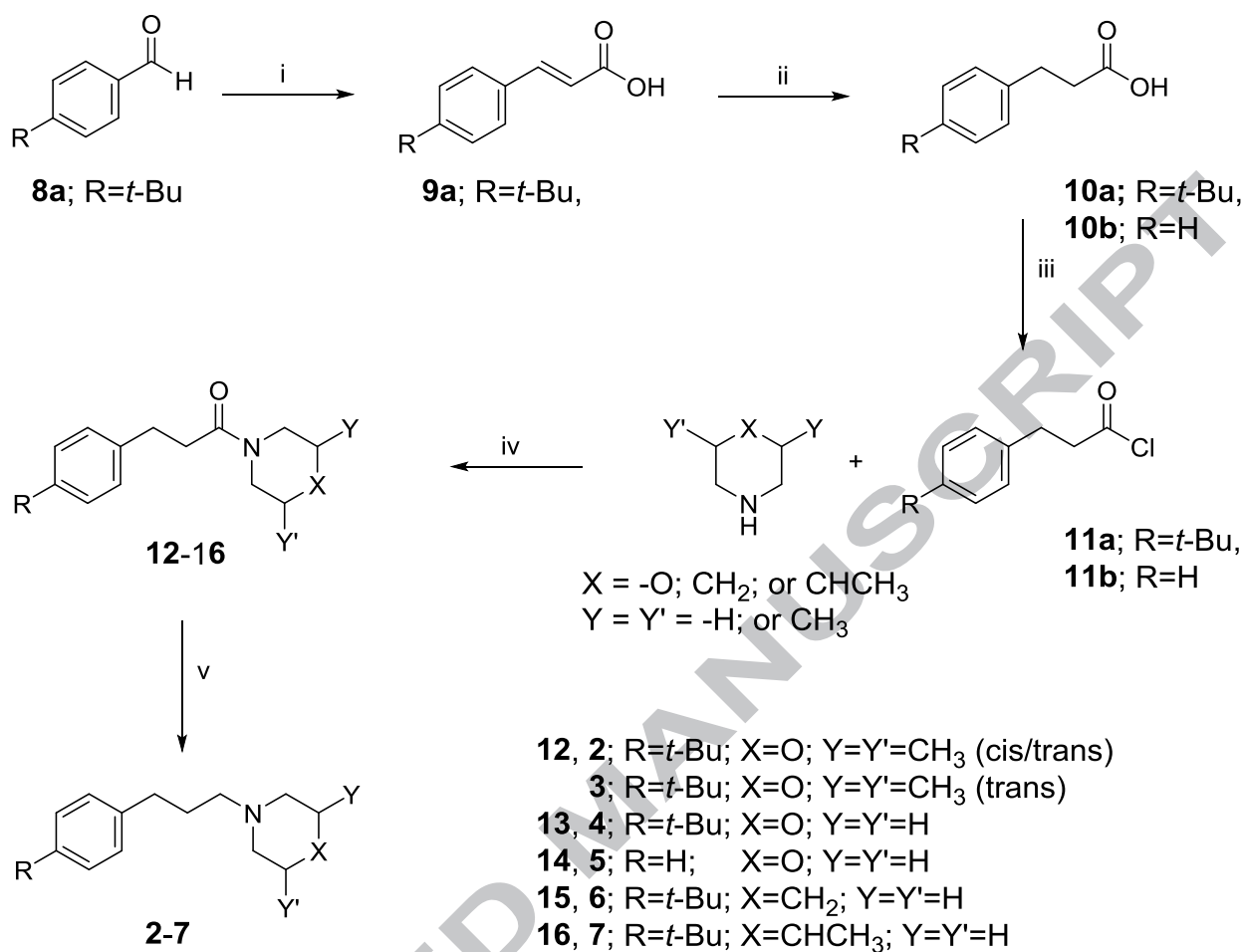
## 2. Results and Discussion

### 2.1. Synthesis

The commercially available free base of fenpropimorph (**1**) was converted to its more water-soluble hydrochloride salt, which had not been previously reported. A series of fenpropimorph analogs was synthesized using a common pathway (Scheme 1). Classical Knoevenagel condensation with the Doebner modification was applied to obtain known 4-*tert*-butyl-phenylacrylic acid (**9a**),<sup>12</sup> using the corresponding commercially available aldehyde **8a** and malonic acid. Catalytic reduction of the olefinic double bond of **9a** with 10% Pd/C under a H<sub>2</sub> atmosphere yielded carboxylic acids **10a**.<sup>13</sup> The acid chlorides **11a** and **11b** were generated in situ from the carboxylic acid **10a** and commercially available

dihydrocinnamic acid (**10b**), respectively, in reaction with thionyl chloride. The acid chlorides were then reacted with the corresponding amine using a literature procedure for a similar compounds<sup>14</sup> to obtain the amides **12-16**, followed by reduction with diborane or a borane dimethyl sulfide complex (in preparation of **7**) to afford the target compounds **2**, and **4-7**. The *trans* isomer **3** was obtained by separation of an isomeric mixture of **2** using flash chromatography. All target compounds were prepared as water-soluble salts. This pathway gave satisfactory yields.

**Scheme 1.** Synthetic pathway for fenpropimorph analogs **2-7**.



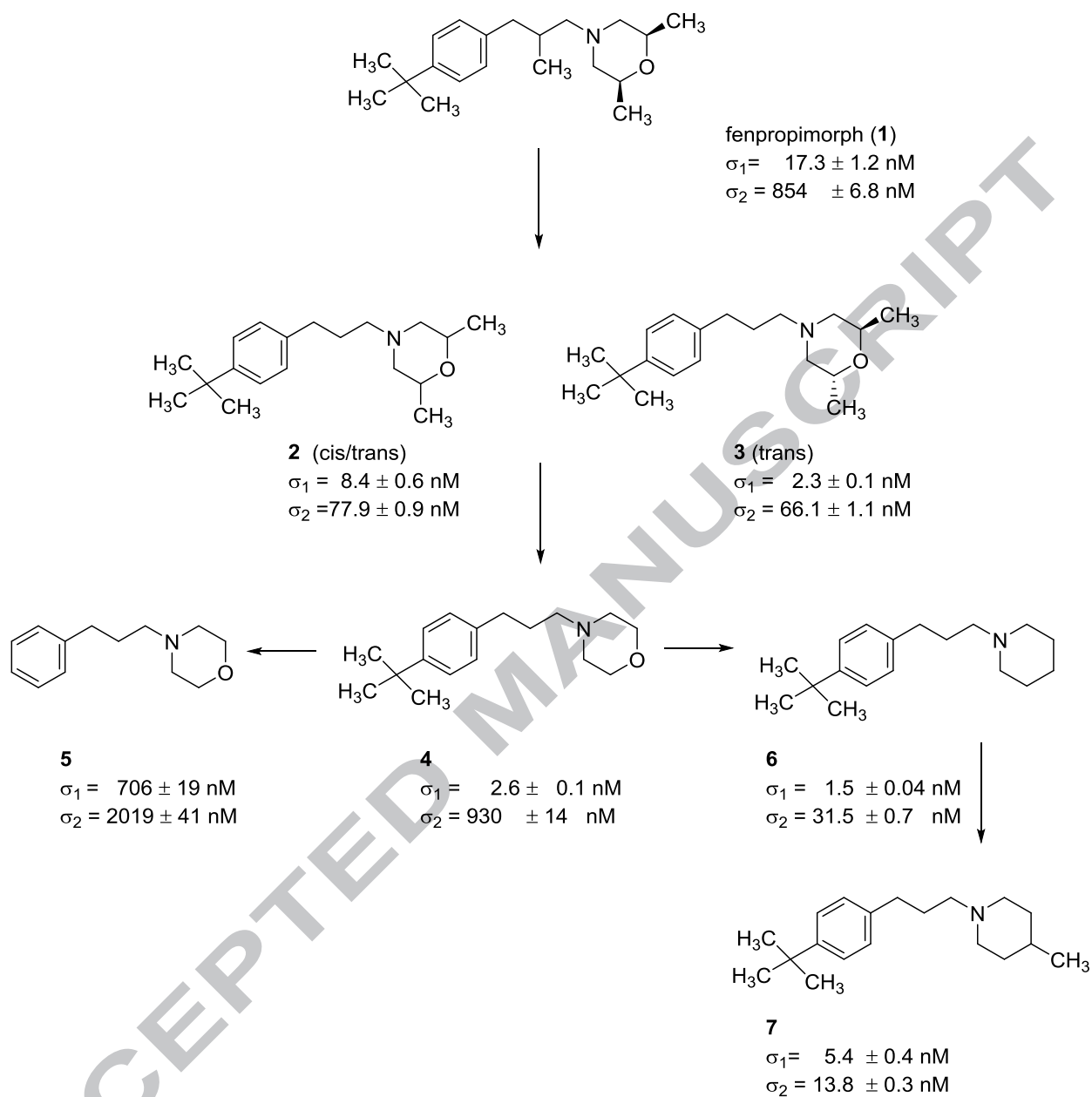
<sup>a</sup>Reagents and conditions: (i) CH<sub>2</sub>(COOH)<sub>2</sub>, piperidine, pyridine; (ii) H<sub>2</sub>, 10% Pd/C, EtOAc; (iii) SOCl<sub>2</sub>; (iv) a.) CH<sub>2</sub>Cl<sub>2</sub>, Et<sub>3</sub>N, stirring at room temperature; b.) 10% HCl, Et<sub>2</sub>O; (v) BH<sub>3</sub>·THF or BH<sub>3</sub>·S(CH<sub>3</sub>)<sub>2</sub> (for **7**), THF, reflux.

The structures of **1-7** were confirmed by <sup>1</sup>H NMR, IR, mp (where appropriate) and C, H, N analysis. The hydrochloride salt of **5** was previously synthesized by a different synthetic route, but was not fully characterized.<sup>15</sup> Compound **6** was not known at the time we prepared it (Scheme 1) but was subsequently reported by Khan and Bhanage<sup>16</sup> using a different method of preparation.

## 2.2. Structure-Affinity Relationship (SAfIR) Studies

$\sigma_1$  receptor binding data and SAfiR are described here in the context of an existing pharmacophore model. The proposed pharmacophore model suggests three major features are important for high binding affinity at  $\sigma_1$  receptors: i) a “primary hydrophobic region” (constituted of aryl ring or similar hydrophobic moiety) situated at 6-10 Å (optimum = 8.3 Å) distant from an amine, ii) a secondary or tertiary amine (the amine can be a part of cyclic structure), and iii) a small “secondary hydrophobic region” distant at 2.4-3.9 Å from the amine (Figure S1).<sup>4, 11</sup>

Fenpropimorph (**1**) seems to meet these structural requirements (Figure S1). That is, the basic tertiary amine of **1** is surrounded by the “primary hydrophobic region” (corresponding to *tert*-butylphenyl; the distance from N atom to the *t*-butyl tertiary C atom = 8.71 Å) and the “secondary hydrophobic region” (the distance from N atom to CH<sub>3</sub> = 3.3 Å).



We assessed the binding affinity of the analogs **1-7** for the  $h\sigma_1$  receptor using [ $^3\text{H}$ ](+)-PTZ as a radioligand and we generated the corresponding binding curves (Figure 2).

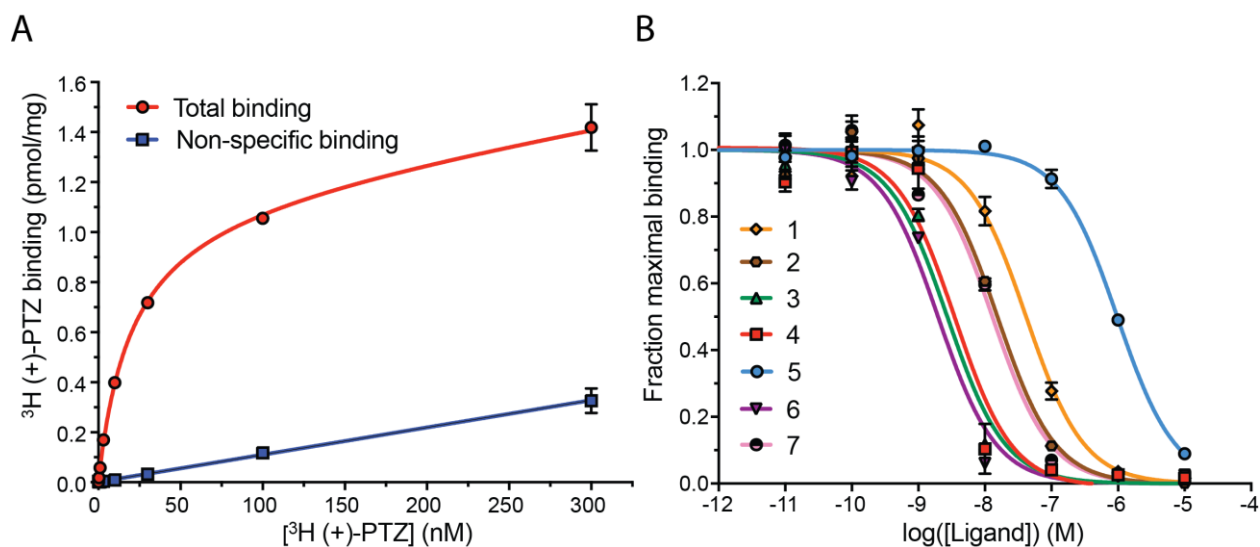


**Figure 2.** Radioligand binding curves for the  $\sigma_1$  receptor. A) A [<sup>3</sup>H](+)-PTZ saturation curve depicting total (red circles) and non-specific (blue squares) binding to *Sf9* membranes.  $K_d \pm \text{SEM} = 20.0 \pm 1.2$  nM. B) Competition binding curve against [<sup>3</sup>H](+)-PTZ in *Sf9* membranes for compounds **1** (orange diamonds), **2** (brown hexagons), **3** (green triangles pointed up), **4** (red squares), **5** (blue circles), **6** (purple triangles pointed down), and **7** (pink half-filled circles).  $K_i$  values are listed in Table 1. Error bars represent SEM. Curves depicted in this figure are representative curves from at least two independent experiments each performed in triplicate.

Compounds **2** and **3** (Table 1), with nearly comparable  $\sigma_1$  receptor affinity, and an affinity at least twice that of **1**, show that the side chain methyl group does not contribute to binding, that the stereochemistry of the morpholine methyl groups are relatively unimportant, and that removal of all the methyl groups (i.e., **4**, Table 1) is tolerated. However, removing the *tert*-butyl group results in a dramatic (i.e., 265-fold) decrease in affinity (i.e., **5**).

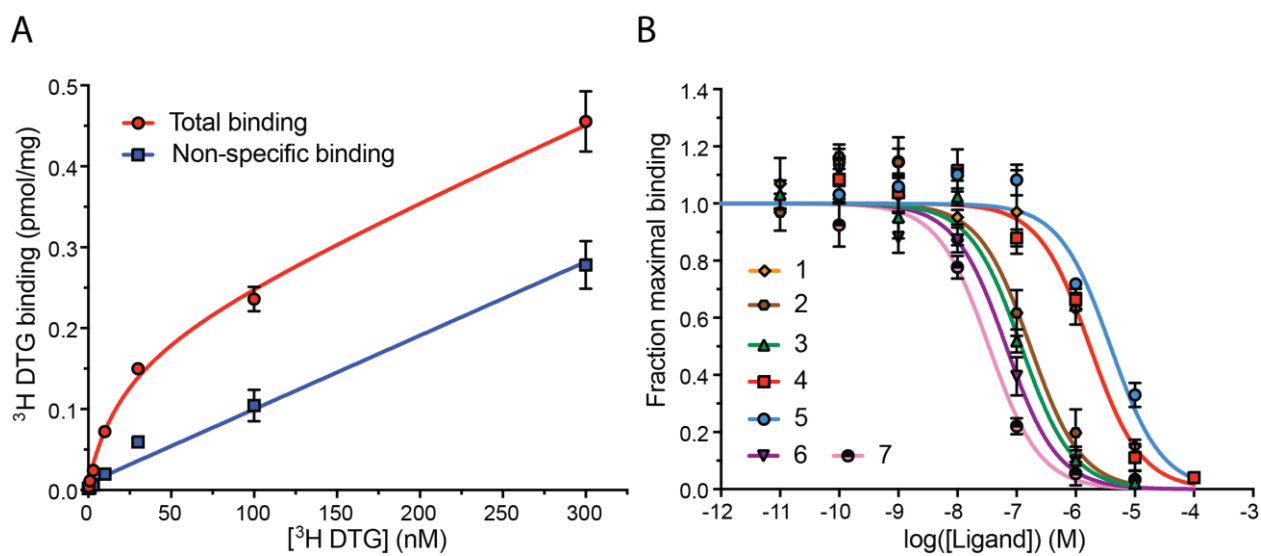
**Table 1.** Binding affinity ( $K_i \pm \text{SEM}$  nM) of fenpropimorph (**1**) and its analogs **2-7** at human  $\sigma_1$  and rat  $\sigma_2$  receptors.

	$K_i^a \pm \text{SEM}$ (nM)		$\sigma_1$ selectivity
	h $\sigma_1$	r $\sigma_2$	
<b>1</b> (fenpropimorph)	17.3 $\pm$ 1.2	854 $\pm$ 6.8	50
<b>2</b>	8.4 $\pm$ 0.6	77.9 $\pm$ 0.9	9
<b>3</b>	2.3 $\pm$ 0.1	66.1 $\pm$ 1.1	29
<b>4</b>	2.6 $\pm$ 0.1	930 $\pm$ 14	360
<b>5</b>	706 $\pm$ 19	2019 $\pm$ 41	3
<b>6</b>	1.5 $\pm$ 0.04	31.5 $\pm$ 0.7	21
<b>7</b>	5.4 $\pm$ 0.4	13.8 $\pm$ 0.3	3

<sup>a</sup>Values presented as the mean  $\pm$  SEM (n = 3)

Removal of the morpholine oxygen atom from **4** (i.e., **6**, Table 1) reveals it to be unimportant for  $\sigma_1$  receptor affinity and, indeed, slightly improves binding affinity. Piperidine analog **6** displays ten times higher affinity than **1**. Elaborated compound **7** (Table 1) possesses structural features required for binding and binds with at least thrice the affinity of **1**.

In addition we monitored the subtype selectivity of analogs **1-7** for  $\sigma_1$  vs  $\sigma_2$  receptors.



Thus, all analogs were examined for their binding affinity at  $\sigma_2$  receptors with [ $^3\text{H}$ ] DTG as a radioligand and binding curves were generated (Figure 3).

**Figure 3.** Radioligand binding curves for the  $\sigma_2$  receptor. A) A [ $^3\text{H}$ ] DTG saturation curve depicting total (red circles) and non-specific (blue squares) binding to PC-12 membranes.  $K_d \pm \text{SEM} = 23.0 \pm 3.9$  nM. B) Competition binding curve against [ $^3\text{H}$ ] DTG in PC-12 membranes for compounds **1** (orange diamonds), **2** (brown hexagons), **3** (green triangles pointed up), **4** (red squares), **5** (blue circles), **6** (purple triangles pointed down), and **7** (pink half-filled circles).  $K_i$  values are listed in Table 1. Error bars represent SEM. Curves depicted in this figure are representative curves from two independent experiments performed in triplicate.

We found that although the morpholine O atom is not important for binding affinity of fenpropimorph analogs at  $\sigma_1$  receptors, its removal resulted in a dramatic decrease in subtype selectivity. For example **4** showed 360-fold selectivity at  $\sigma_1$  receptors compared to  $\sigma_2$  receptors, whereas its piperidine counterpart **6** is only 21-fold selective for  $\sigma_1$  receptors compared to  $\sigma_2$  receptors.

### 2.3. Molecular Modeling

The two high-resolution crystal structures of the  $\sigma_1$  receptor (PDB ID: 5HK1 and 5HK2)<sup>7</sup> served as excellent starting points for our docking studies. Since the conformation of the receptor was highly similar for the antagonist and the agonist/inverse agonist-bound forms, we conducted our docking studies on the higher resolution antagonist-bound crystal structure (PDB ID: 5HK1) of the  $h\sigma_1$  receptor. The binding site, as identified by Schmidt et al.,<sup>7</sup> consists primarily of hydrophobic residues with the exception of two acidic residues, Glu172 and Asp126. We utilized the glutamate residue (Glu172), previously shown to be important for binding by mutagenesis data,<sup>17</sup> to dock our compounds in a spherical region of 6 Å radius. To quantify the interactions observed between the ligands and the receptor, we

performed a Hydrophatic INTeractions (HINT) analysis that takes into account all non-covalent interactions between two molecules.<sup>18</sup> A higher HINT score implies a more favorable interaction between the two (i.e., the receptor and a ligand in this case).<sup>18</sup>

ACCEPTED MANUSCRIPT

The SAfiR studies indicated that none of the methyl substituents on fenpropimorph (**1**) contribute to its affinity at the  $h\sigma_1$  receptor. Thus, we docked analog **4** ( $K_i = 2.6$  nM) and

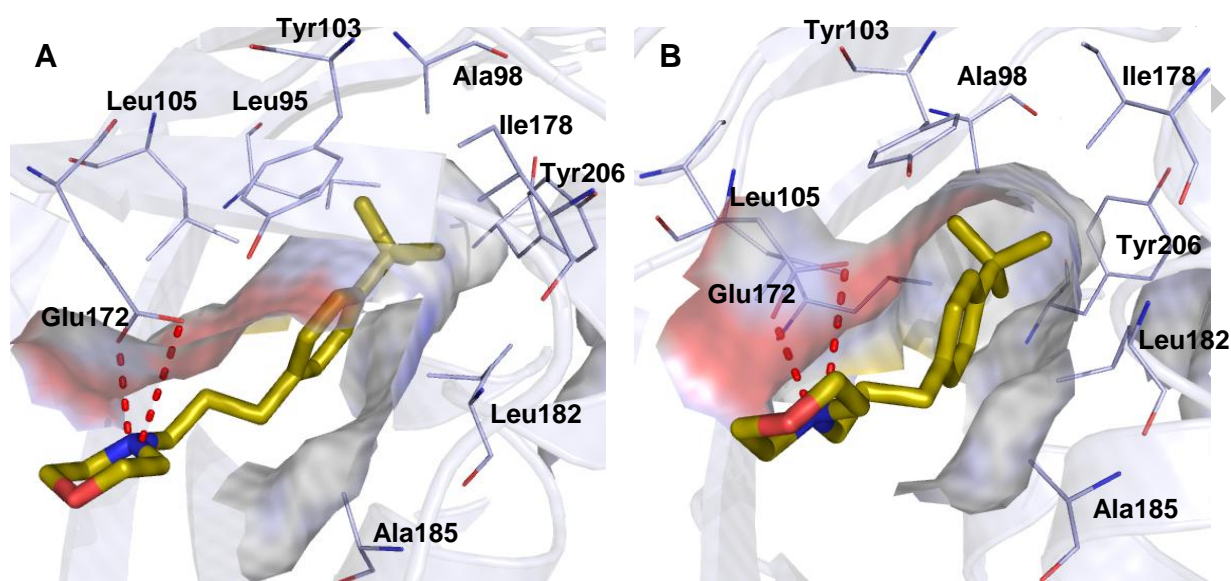


**Figure 4.** Two views of analog **4** (yellow capped sticks) docked in the binding site of the  $h\sigma_1$  receptor (PDB ID: 5HK1). **A)** The amino acid residues of the crystal structure are shown as pale blue-capped sticks. The N atom of the morpholine ring of analog **4** appears to be involved in a bidentate ionic interaction (dashed red lines) with the O atoms of the carboxylate group of Glu172. **B)** The 4-*tert*-butyl group is surrounded by and interacting with hydrophobic residues – Leu95, Ala98, Tyr103, Leu105, Ile178, Leu182, Ala185 and Tyr206 – at the binding site.

found that the 4-*tert*-butylphenyl group occupied a pocket consisting of hydrophobic residues – Leu95, Ala98, Tyr103, Leu105, Ile178, Leu182, Ala185 and Tyr206, whereas the morpholine nitrogen atom formed a key bidentate ionic interaction with the carboxylate O atoms of Glu172 (Figures 4 A and B). The lower-affinity des 4-*tert*-butyl analog **5** ( $K_i = 706$  nM) lacks these extensive hydrophobic interactions of **4** and appears to be oriented in the opposite direction (Figure S2). Analog **5** did show weak hydrophobic interactions with Val152 and Ala185 while retaining the key bidentate interaction with Glu172 (Figure S2). HINT analysis of the solution representing its binding mode might potentially explain the ~265-fold difference in the affinity of **5** as compared to **4** (Table 1) at  $h\sigma_1$  receptors.

In our biological studies we examined racemic fenpropimorph (**1**) and because radioligand binding affinity data for (*R*)- and (*S*)-fenpropimorph are lacking we docked both isomers. Both, the (*R*)- and (*S*)-isomer of **1** mimicked the binding mode of **4**. In both cases, the bidentate interactions of the N atom with the O atoms of the carboxylate group of Glu172 as well as the hydrophobic interactions of the 4-*tert*-butylphenyl group were retained both by the (*R*)- and (*S*)-isomer of **1** (Figure S3). The HINT scores for the two isomers, (*R*)- and (*S*)-**1**, were comparable (Table 2) suggesting that the stereocenter might not be significantly important for binding. This is supported by our biological data.

**Table 2.** Summary of HINT scores for the deconstructed analogs **4**, **5** and the (*R*)- and (*S*)-fenpropimorph docked in the binding site of the  $\sigma_1$  receptor.

Ligand	Total HINT score <sup>a</sup>	Total hydrophobic <sup>b</sup>	Total polar <sup>c</sup>	Hydrophobic <sup>d</sup>
<b>4</b>	<b>2041</b>	905	1136	1828
<b>5</b>	<b>394</b>	-756	1150	488
( <i>R</i> )-Fenpropimorph ( <b>1</b> )	<b>1346</b>	149	1197	1968
( <i>S</i> )-Fenpropimorph ( <b>1</b> )	<b>1592</b>	323	1269	2111

<sup>a</sup>Sum of all noncovalent interactions including hydrophobic and polar interactions between two entities,<sup>18</sup> <sup>b</sup>sum of hydrophobic and hydrophobic/polar (which represent desolvation energy) interactions,<sup>18</sup> <sup>c</sup>sum of attractive acid/base and hydrogen bond interactions and repulsive acid/acid and base/base interactions,<sup>18</sup> <sup>d</sup>sum of hydrophobic interactions between individual atoms of the ligand and the receptor<sup>18</sup>

To understand the >3500-fold difference in the binding affinity of fenpropimorph (**1**) at guinea pig vs human orthologues of the  $\sigma_1$  receptor, we aligned amino acid sequences of both orthologues and examined their sequence identity in the orthosteric binding site (Figure

S4). It appears that the orthosteric binding sites in both species are highly conserved and there are no differences in the amino acid sequences that might explain the extremely high affinity of fenpropimorph (**1**) at guinea pig relative to human  $\sigma_1$  receptors. Differences in results might be related to experimental differences in the radioligand binding procedures.

Our docking studies and HINT analysis are in agreement with our biological data which suggests that the chiral center on the 2-methylpropyl linker, the 3,5-dimethyl groups, and the oxygen atom of the morpholine ring might not be important for binding affinity of fenpropimorph at human  $\sigma_1$  receptors.

### 3. Conclusions

Fenpropimorph (**1**) does not bind at human  $\sigma_1$  receptors with nearly the same affinity it display for  $\sigma_1$  receptors of other species. Nevertheless, even with lower affinity for h $\sigma_1$  receptors, it is still 50-fold selective for  $\sigma_1$  vs  $\sigma_2$  receptors. The present findings demonstrate that: i) phenpropimorph binds at human  $\sigma_1$  receptors with much lower affinity than its reported affinity for guinea pig  $\sigma_1$  receptors, ii) the side chain methyl group of **1** is not required for  $\sigma_1$  binding, iii) the lipophilic character on the “left hand” portion of the molecule (as drawn here) contributes to binding, iv) the stereochemistry about the morpholine methyl substituents is unimportant, and that v) the morpholine oxygen atom does not contribute to (and might even detract from)  $\sigma_1$  receptor binding.

In addition, given the availability of the human  $\sigma_1$  receptor crystal structure we, for the first time, are able to provide support for Glennon’s pharmacophore model at an atomic level.

Alignment of amino acid sequences for the human versus guinea pig orthologs of the  $\sigma_1$  receptor could not explain the differences in affinities observed for fenpropimorph. Docking

studies and HINT analysis indicated that the high-scoring ionic interactions with Glu172, retained by all analogs, might be a contributing factor for their high affinity for the  $\sigma_1$  receptor. HINT analysis further indicated a high degree of contribution by hydrophobic interactions with the amino acid residues of the binding site and might point towards the necessity of the 4-*t*-butylphenyl group for the binding of fenpropimorph. Our current findings also show that fenpropimorph (**1**) does not bind with nearly the high affinity for human  $\sigma_1$  receptors that it displays for other species (e.g. guinea pig), and that this must be taken in consideration for future studies with fenpropimorph analogs. Nevertheless, simplified fenpropimorph analogs such as **4** and **5** are worthy of continued studies. Most interesting, perhaps, is that **4**, is >350-fold selective for  $\sigma_1$  vs  $\sigma_2$  receptor binding.

In summary, our findings support and confirm a previously proposed  $\sigma_1$  receptor pharmacophore;<sup>11</sup> and, with respect to compound **4**, suggest it might be a suitable template for exploitation to develop compounds with significant  $\sigma_1$  versus  $\sigma_2$  receptor selectivity.

## 4. Experimental section

### 4.1. Synthesis

All solvents and reagents used were purchased from Sigma-Aldrich. Routine thin layer chromatography (TLC) was performed on silica gel GHLF plates (250  $\mu$ , 2.5 x 10 cm; Analtech Inc. Newark, DE) and examined by UV (model UVGL-25 mineralight lamp, multiband UV –  $\lambda = 254/365$  nm (UVP, Upland, CA). TLC plates were also developed using an iodine chamber containing a few crystals of iodine mixed with silica. Chromatographic separations were performed on silica gel columns (Silica Gel 62, 60-200 mesh, 150  $\text{\AA}$ , Sigma-Aldrich). Flash chromatography was performed on a CombiFlash Companion/TS Teledyne Isco Inc. (Lincoln, NE) instrument using normal phase silica flash chromatography

columns (35-70  $\mu$ , mesh 230-400, 60  $\text{\AA}$ , RediSep). Melting points were determined in glass capillary tubes on a Thomas-Hoover<sup>®</sup> melting point apparatus and are uncorrected.

Hydrogenation reactions were performed using an hydrogenation apparatus (4833/3900 apparatus, Parr Instrument Company, Moline, IL). <sup>1</sup>H NMR spectra were recorded with a Varian EM-390 300 MHz with tetramethylsilane (TMS) as an internal standard. Peak positions are reported in parts per million ( $\delta$ ). Elemental analyses were performed by Atlantic Microlab Inc. (Norcross, GA) for the indicated elements and results are within 0.4 % of calculated values.

Compounds **9a**<sup>12</sup> and **10a**<sup>13</sup> were prepared according to literature procedures.

**4.1.1. Fenpropimorph Hydrochloride (1).** Fenpropimorph was purchased from Sigma-Aldrich and converted to its HCl salt. The resulting solid was recrystallized from Et<sub>2</sub>O/MeOH yielding a white crystalline product: mp 220-222 °C. <sup>1</sup>H NMR (DMSO-d<sub>6</sub>)  $\delta$  0.91 (d,  $J$  = 6 Hz, 3H, CH<sub>3</sub>), 1.11 (m, 6H, CH<sub>3</sub>), 1.27 (s, 9H, CH<sub>3</sub>), 2.3 (m, 2H, CH<sub>2</sub>), 2.53 (m, 1H, CH), 2.58 (m, 2H, CH<sub>2</sub>), 3 (m, 2H, CH<sub>2</sub>), 3.45 (m, 2H, CH<sub>2</sub>), 4.08 (m, 2H, CH), 7.16 (d,  $J$  = 12 Hz, 2H, CH), 7.32 (d,  $J$  = 12 Hz, 2H, CH). Anal. Calcd for (C<sub>20</sub>H<sub>33</sub>NO·HCl): C = 70.66%, H = 10.08%, N = 4.12%. Actual: C = 70.50%, H = 10.23%, N = 4.11%.

**4.1.2. 4-[3-[(4-*tert*-Butylphenyl)propyl]-2,6-dimethylmorpholine Hydrochloride (2).**

Diborane-THF complex (11.5 mL) was added in a dropwise manner to a solution of **12** (2 g, 0.01 mol) in dry THF (10 mL) at 0 °C under a N<sub>2</sub> atmosphere. The reaction mixture was heated at reflux for 3 h. A solution of 10% HCl (20 mL) was added in a dropwise manner at 0 °C to the reaction mixture, which was then heated at reflux for additional 15 h. The solvent was removed under reduced pressure. The reaction was basified to pH 10 by the addition of 2% NaOH solution and the mixture was extracted with Et<sub>2</sub>O (3 x 20 mL). The Et<sub>2</sub>O solution

was dried ( $\text{Na}_2\text{SO}_4$ ), filtered, and the solvent evaporated under reduced pressure. An  $\text{Et}_2\text{O}$  solution of the residue was treated with a solution of  $\text{Et}_2\text{O}/\text{HCl}$  and the resultant precipitate was collected by filtration, washed well with  $\text{Et}_2\text{O}$ , and recrystallized from an anhydrous  $\text{Et}_2\text{O}/\text{MeOH}$  mixture to yield 1.86 g (93%) of **2** as white crystals as a mixture of cis and trans isomers: mp 230 – 244 °C.  $^1\text{H}$  NMR ( $\text{DMSO}-d_6$ )  $\delta$  1.11 (d,  $J = 6$  Hz, 6H,  $\text{CH}_3$ ), 1.27 (s, 9H,  $\text{CH}_3$ ), 1.43 (m, 2H,  $\text{CH}_2$ ), 2.1 (m, 2H,  $\text{CH}_2$ ), 2.51 (m, 2H,  $\text{CH}_2$ ), 2.6 (m, 2H,  $\text{CH}_2$ ), 3.1 (m, 2H,  $\text{CH}_2$ ), 3.4 (m, 2H, CH), 7.16 (d,  $J = 6$  Hz, 2H, CH), 7.32 (d,  $J = 6$  Hz, 2H, CH). Anal. Calcd for ( $\text{C}_{19}\text{H}_{31}\text{NO}\cdot\text{HCl}$ ): C = 70.02%, H = 9.90%, N = 4.30%. Actual: C = 70.14%, H = 10.04%, N = 4.30%.

#### 4.1.3. Trans-4-[3-[(4-*tert*-Butylphenyl)propyl]-2,6-dimethylmorpholine Hydrochloride

(**3**). A part of the isomeric mixture (free base) **2** (0.2 g, 0.001 mol) was separated using silica gel flash chromatography (hexane-EtOAc = 9:1) to give a yellow oil which was treated with a solution of  $\text{Et}_2\text{O}/\text{HCl}$ . The resultant precipitate was collected by filtration, washed well with anhydrous  $\text{Et}_2\text{O}$  and recrystallized from an  $\text{Et}_2\text{O}/\text{MeOH}$  mixture to yield 0.11 g (56%) of **3** as white crystals: mp 248-249 °C.  $^1\text{H}$  NMR ( $\text{DMSO}-d_6$ )  $\delta$  1.10 (d,  $J = 6$  Hz, 6H,  $\text{CH}_3$ ), 1.25 (s, 9H,  $\text{CH}_3$ ), 1.99 (m, 3H,  $\text{CH}_2$ ), 2.57 (m, 4H,  $\text{CH}_2$ ), 2.99 (m, 3H,  $\text{CH}_2$ ), 3.89 (m, 2H, CH), 7.13 (d,  $J = 9$  Hz, 2H, CH), 7.29 (d,  $J = 9$  Hz, 2H, CH). Anal. Calcd for ( $\text{C}_{19}\text{H}_{31}\text{NO}\cdot\text{HCl}$ ): C = 70.02%, H = 9.90%, N = 4.30%. Actual: C = 70.27%, H = 9.91%, N = 4.29%.

Analogs **4-6** were obtained following the procedure for the preparation of **2** from amides **13-15**, respectively.

#### 4.1.4. 4-[3-(4-*tert*-Butylphenyl)propyl]-morpholine Oxalate (**4**).

White crystals: mp 176-178 °C (Et<sub>2</sub>O/MeOH). Yield 0.07 g (14%). <sup>1</sup>H NMR (DMSO-d<sub>6</sub>) δ 1.25 (s, 9H, CH<sub>3</sub>), 1.89 (m, 2H, CH<sub>2</sub>), 2.55 (m, 2H, CH<sub>2</sub>), 2.7-3.1 (m, 6H, CH<sub>2</sub>), 3.74 (m, 4H, CH<sub>2</sub>), 7.12 (d, *J* = 9 Hz, 2H, CH), 7.28 (d, *J* = 6, 2H, CH). Anal. Calcd for (C<sub>17</sub>H<sub>27</sub>NO·C<sub>2</sub>H<sub>2</sub>O<sub>4</sub>): C = 64.93%, H = 8.32%, N = 3.99. Actual: C = 64.77%, H = 8.17%, N = 3.94%.

#### 4.1.5. 4-(3-Phenylpropyl)-morpholine Hydrochloride (5).

White crystals: mp 137-138 °C (*i*-PrOH/Et<sub>2</sub>O). Yield 0.05 g (7%). <sup>1</sup>H NMR (DMSO-d<sub>6</sub>) δ 2.02 (m, 2H, CH<sub>2</sub>), 2.49 (m, 2H, CH<sub>2</sub>), 2.62 (t, *J* = 6 Hz, 2H, CH<sub>2</sub>), 3.03 (m, 4H, CH<sub>2</sub>), 3.89-3.80 (m, 4H, CH<sub>2</sub>), 7.24 (m, 5H, CH), 11.12 (s, 1H, NH<sub>3</sub><sup>+</sup>). Anal. Calcd for (C<sub>13</sub>H<sub>19</sub>NO·HCl): C = 64.59%, H = 8.34%, N = 5.79%. Actual: C = 64.46%, H = 8.37%, N = 5.78%.

#### 4.1.6. 4-[3-(4-*tert*-Butylphenyl)propyl]-piperidine Oxalate (6).

White crystals: mp 177-179 °C (Et<sub>2</sub>O/MeOH). Yield 0.16 g (4.5%). <sup>1</sup>H NMR (DMSO-d<sub>6</sub>) δ 1.26 (s, 9H, CH<sub>3</sub>), 1.5 (m, 2H, CH<sub>2</sub>), 1.71 (m, 4H, CH<sub>2</sub>), 1.93 (m, 2H, CH<sub>2</sub>), 2.51 (t, 2H, CH<sub>2</sub>), 2.57 (t, 2H, CH<sub>2</sub>), 2.97 (t, 2H, CH<sub>2</sub>), 3.08 (m, 2H, CH<sub>2</sub>), 7.15 (d, *J* = 6 Hz, 2H, CH), 7.31 (d, *J* = 6 Hz, 2H, CH). Anal. Calcd for (C<sub>18</sub>H<sub>29</sub>NO·C<sub>2</sub>H<sub>2</sub>O<sub>4</sub>): C = 68.74%, H = 8.94%, N = 4.01%. Actual: C = 68.45%, H = 9.08%, N = 3.94%.

#### 4.1.7. 4-[3-(4-*tert*-Butylphenyl)propyl]-4-methylpiperidine Oxalate (7).

Borane dimethyl sulfide complex (0.9 mL) was added in a dropwise manner to a solution of **16** (1.65 g, 0.006 mol) in dry THF (25 mL) at 0 °C under a N<sub>2</sub> atmosphere. The reaction mixture was heated at reflux for 3 h. An aqueous solution of 10% HCl (20 mL) was added in a dropwise manner at 0 °C to the reaction mixture which was then heated at reflux for additional 15 h. The solvent was removed under reduced pressure. The reaction mixture was

basified to pH 10 by adding 2% aqueous NaOH solution and the mixture was extracted with Et<sub>2</sub>O (3 x 40mL). The Et<sub>2</sub>O solution was dried (Na<sub>2</sub>SO<sub>4</sub>) and evaporated under reduced pressure. The free base of **7** was dissolved in anhydrous Et<sub>2</sub>O and treated with a solution of oxalic acid. The resultant precipitate was collected by filtration, washed well with anhydrous Et<sub>2</sub>O, and recrystallized from a Et<sub>2</sub>O/MeOH mixture to yield 0.22 g (13%) of **7** as white crystals: mp 168-176 °C. <sup>1</sup>H NMR (DMSO-d<sub>6</sub>) δ 0.92 (d, *J* = 6.44 Hz, 3H, CH<sub>3</sub>), 1.26 (s, 9H, CH<sub>3</sub>), 1.6 (m, 1H, CH), 1.77 (m, 2H, CH<sub>2</sub>), 1.91 (m, 2H, CH<sub>2</sub>), 2.5 (m, 2H, CH<sub>2</sub>), 2.58 (t, 2H, CH<sub>2</sub>), 2.97 (t, 2H, CH<sub>2</sub>), 2.98 (m, 2H, CH<sub>2</sub>), 3.38 (m, 2H, CH<sub>2</sub>), 7.15 (d, *J* = 8 Hz, 2H, CH), 7.32 (d, *J* = 8 Hz, 2H, CH). Anal. Calcd for (C<sub>19</sub>H<sub>31</sub>N·C<sub>2</sub>H<sub>2</sub>O<sub>4</sub>): C = 69.39%, H = 9.15%, N = 3.81%. Actual: C = 69.13%, H = 9.04%, N = 3.81%.

#### 4.1.8. 3-(4-*tert*-Butyl)phenyl propanoyl chloride (**11a**).

Compound **10a** (3.81 g, 0.02 mol) was dissolved in dry benzene (5 mL, 0.06 mol) at room temperature then SOCl<sub>2</sub> (10 mL, 0.14 mol) was added in a dropwise manner. The reaction mixture was heated at reflux for 15 h. The solvent was evaporated under reduced pressure to give **11a** (4.49 g, 95%) as a yellow oil. The crude product was used in the next step without further purification or characterization.

#### 4.1.9. 3-Phenylpropanoyl chloride (**11b**).

Dihydrocinnamic acid (**10b**) (3.0 g, 0.02 mol) was dissolved in dry benzene (5 mL, 0.06 mol) at room temperature then SOCl<sub>2</sub> (10 mL, 0.14 mol) was added in a dropwise manner. The reaction mixture was allowed to heat at reflux for 4 h. The solvent was evaporated under reduced pressure to give (3.4 g, 95%) of **11b** as yellow oil. The crude product was used in the next step without further purification or characterization.

**4.1.10. 3-(4-*tert*-Butyl)-phenyl-1-(2,6-dimethylmorpholinyl)propan-1-one (12).**

A solution of 3-(4-*tert*-butyl)-3-phenylpropanoyl chloride (**11a**) (2.83 g, 0.01 mol) in dry CH<sub>2</sub>Cl<sub>2</sub> (10 mL) was added in a dropwise manner to a stirred solution of 2,6-dimethylmorpholine (1.86 mL, 0.02 mol), TEA (3.45 mL, 0.03 mol), and dry CH<sub>2</sub>Cl<sub>2</sub> (20 mL). The reaction mixture was allowed to stir at room temperature for 15 h. The solvent was evaporated under reduced pressure. A solution of 10% HCl (20 mL) was added to the oily residue. The mixture was washed with Et<sub>2</sub>O (3 x 20 mL). The Et<sub>2</sub>O portion was dried (Na<sub>2</sub>SO<sub>4</sub>) and the solvent was removed under reduced pressure to give (2.00 g, 56%) of **12** as a yellow oil. The crude product was used in the next step without further purification or characterization.

Amides **13-16** were obtained using a procedure similar to that used for **12**.

**4.2. Biological studies**Recombinant receptor expression

Human  $\sigma_1$  receptors were expressed in *Sf9* insect cells as described previously.<sup>7</sup> In short, the human  $\sigma_1$  receptor was cloned into the pFastBac vector and expressed using the baculovirus expression system. Cells were grown in a shaker at 27° C, and infected when cells reached a density of 4 x 10<sup>6</sup> cells/mL. At 48 hours post-infection, cells were harvested by centrifugation and used for membrane preparation.

Preparation of cell membranes for radioligand binding experiments

Membranes were prepared from PC-12 (for  $\sigma_2$  binding) or *Sf9* (for  $\sigma_1$  binding) cells with a protocol based on that of Vilner *et al.*<sup>19</sup> In summary, PC-12 cells were washed with ice cold PBS and harvested with a cell scraper and *Sf9* cells were pelleted by centrifugation. Cell pellets were suspended in 20 mM HEPES pH 7.5 supplemented with cComplete Mini, EDTA-

free Protease Inhibitor Cocktail Tablets (Roche, 1 tablet per 50 mL buffer). The cells were homogenized using a needle and syringe, and then centrifuged at 50,000 x g for 20 min. The supernatant was discarded and the membranes were resuspended in cold 50 mM Tris pH 8.0 containing cOmplete Mini, EDTA-free Protease Inhibitor Cocktail Tablets (Roche, 1 tablet per 50 mL buffer). The membranes were again centrifuged at 50,000 x g for 20 min, and then resuspended in 1-5 mL of the same Tris/protease inhibitor buffer. Total protein content was measured using the Biorad DC protein assay according to the manufacturer's instructions. Membranes divided into 200  $\mu$ L aliquots, flash frozen, and stored at  $-80^{\circ}$  C until use.

#### Radioligand saturation binding

Both  $\sigma_1$  and  $\sigma_2$  receptor radioligand saturation binding to membranes was determined using an assay similar to that described by Chu and Ruoho,<sup>20</sup> with minor differences. Briefly, membranes from infected *Sf9* insect cells (2.5  $\mu$ g total protein per reaction) and 0 - 300 nM  $^3$ H(+)-PTZ for  $\sigma_1$  binding assays, or PC-12 cells (15-30  $\mu$ g total protein per reaction) 0 - 30 nM  $^3$ H-ditolylguanidine (DTG) for  $\sigma_2$  binding assays, were incubated in a 100  $\mu$ L reaction buffered with 50 mM Tris pH 8.0. In the  $\sigma_2$  binding assays, concentrations of 100 and 300 nM DTG were assayed by isotopic dilution to minimize use of  $^3$ H-DTG, and  $\sigma_1$  receptor sites were blocked by the addition of 1.8  $\mu$ M (+)-SKF-10,047. For each saturation curve, a second curve that was otherwise identical save for the addition of 2  $\mu$ M haloperidol was measured in parallel to determine nonspecific binding. Reactions were incubated on a shaker at 37  $^{\circ}$ C for 90 min and then terminated via filtration through glass fiber filters using a Brandel cell harvester. Glass fiber filters were soaked in 0.3% polyethylenimine for at least 20 min at room temperature prior to harvesting. After washing, filters were soaked in 5 mL Cytoscint scintillation fluid overnight and measured on a Beckman Coulter LS 6500 scintillation counter the next morning.  $K_d$  values were calculated using non-linear regression tools from

Graphpad Prism version 7.0b.

### Competition binding assays

Radioligand competition curves testing the binding of compounds **1-7** to both  $\sigma_1$  and  $\sigma_2$  receptors were performed similarly to what has been described by Chu and Ruoho,<sup>20</sup> with slight modifications. For  $\sigma_1$  receptor competition curves, *Sf9* insect membranes overexpressing  $\sigma_1$  receptor (2.5  $\mu\text{g}$  of total protein per reaction) were incubated in a 100  $\mu\text{L}$  reaction buffered with 50 mM Tris pH 8.0, with 10 nM  $^3\text{H}(+)\text{-PTZ}$  and 8 concentrations ranging from 10 pM – 100  $\mu\text{M}$  of the competing cold ligand. For  $\sigma_2$  receptor competition curves, PC-12 membranes (12-30  $\mu\text{g}$  total protein per reaction) were incubated in the same volume with the same buffer and 30 nM  $^3\text{H}$  DTG and 1.8  $\mu\text{M}$  (+)SKF-10,047 to block  $\sigma_1$  receptor binding sites. As in the saturation curves, reactions were incubated for 90 min at 37  $^\circ\text{C}$ , and were then terminated by filtration through a glass fiber filter using a Brandel cell harvester. Glass fiber filters were soaked in 0.3% polyethylenimine for at least 20 min at room temperature prior to harvesting. All curves were assessed by two or three independent experiments performed in triplicate. After the filters were washed, they were soaked in 5 mL of Cytoscint scintillation fluid overnight and radioactivity was measured using a Beckman Coulter LS 6500 scintillation counter.  $K_i$  values were computed directly without the use of the Cheng-Prusoff correction using Graphpad Prism version 7.0b software.

### **4.3. Molecular modeling**

The X-ray crystal structure of the  $\sigma_1$  receptor co-crystallized with PD144418 was retrieved from the Protein DataBank (PDB ID: 5HK1).<sup>7</sup> Only a single monomer of the receptor (chain B) was retained for the docking studies. The ligands, including PD144418, were sketched and energy minimized using Tripos Force Field and Gasteiger-Hückel charges in SYBYL X-2.1

(Tripos International). For the purpose of the docking studies, we utilized GOLD suite 5.2<sup>21</sup> to define a spherical region of radius 6 Å around the amino acid Glu172 with each ligand being docked 30 times in the binding site and early termination switched off. The solutions generated were analyzed on the basis of GOLD score and selected ligand-receptor complexes were energy minimized in SYBYL X-2.1 (Tripos International). HINT analysis<sup>18</sup> was performed in SYBYL 8.1 (Tripos International) with all parameters set at default and the output examined to arrive at HINT scores.

### **Acknowledgements**

We thank Prof. Richard A. Glennon for discussions and proof-reading the manuscript. We thank Prof. Simona Collina for sponsoring Elena Sguazzini to conduct her research at VCU as an exchange student from the University of Pavia, Italy. Kavita A. Iyer is the recipient of a Lowenthal Award (2013-2015). We acknowledge support to A.C.K. from the Vallee Foundation, the Esther A. and Joseph Klingenstein Fund, and the Harvard Brain Initiative Winthrop Fund.

### **Supplementary data**

Supplementary data associated with this article can be found, in the online version, at...

### **References and notes**

1. Su TP, Hayashi T, Maurice T, Buch S, Ruoho AE. The sigma-1 receptor chaperone as an inter-organelle signaling modulator. *Trends Pharmacol Sci.* 2010; 31: 557-566.
2. Mavlyutov TA, Guo LW, Epstein ML, Ruoho AE. Role of the Sigma-1 receptor in Amyotrophic Lateral Sclerosis (ALS). *J Pharmacol Sci.* 2015; 127: 10-16.
3. Li Volti G, Murabito P. Sigma-1 receptor and neuroprotection: current outlook and potential therapeutic effects. *Neural Regen Res.* 2016; 11: 1392-1393.
4. Matsumoto RR, Bowen WD, Su T-P. *Sigma Receptors, Chemistry, Cell Biology and Clinical Implications.* New York, NY: Springer; 2007.
5. Quirion R, Bowen WD, Itzhak Y, Junien JL, Musacchio JM, Rothman RB, Su TP, Tam SW, Taylor DP. A proposal for the classification of sigma binding sites. *Trends Pharmacol Sci.* 1992; 13: 85-86.
6. Hanner M, Moebius FF, Flandorfer A, Knaus, HG, Striessnig J, Kempner E, Glossmann H. Purification, molecular cloning, and expression of the mammalian sigma1-binding site. *Proc Natl Aca. Sci. USA* 1996; 93: 8072-8077.
7. Schmidt HR, Zheng S, Gurpinar E, Koehl A, Manglik A, Kruse AC. Crystal structure of the human  $\sigma_1$  receptor. *Nature* 2016; 532: 527-530.

8. Moebius FF, Bermoser K, Reiter RJ, Hanner M, Glossmann H. Yeast sterol C-C isomerase: identification and characterization of a high affinity binding site for enzyme inhibitors. *Biochemistry* 1996; 35: 16871-16878.
9. Moebius FF, Reiter RJ, Hanner M, Glossmann H. High affinity of sigma<sub>1</sub>-binding sites for sterol isomerization inhibitors: evidence for a pharmacological relationship with the yeast sterol C<sub>8</sub>-C<sub>7</sub> isomerase. *Brit J Pharmacol.* 1997; 121: 1-6.
10. Hajipour AR, Fontanilla D, Chu UB, Arbabian M, Ruoho AE. Synthesis and characterization of N,N-dialkyl and N-alkyl-N-aralkyl fenpropimorph-derived compounds as high affinity ligands for sigma receptors. *Bioorg Med Chem.* 2010; 18: 4397-4404.
11. Glennon RA. Pharmacophore identification for sigma-1 ( $\sigma_1$ ) receptor binding: application of the “deconstruction-reconstruction-elaboration” approach. *Mini-reviews in Med. Chem.* 2005; 5: 927-940.
12. Tsatsas G, Psarrea-Sandris A, Sandris C, Valiraki A. Synthesis and pharmacodynamic activity of cinnamic acid derivatives. III. p-Alkylcinnamic acids. *Bull Soc Chim Fr.* 1964; 10: 2615-2617.
13. Matasi JJ, Caldwell JP, Hao J, Neustadt B, Arik L, Foster CJ, Lachowicz J, Tulshian DB. The discovery and synthesis of novel adenosine receptor (A<sub>2A</sub>) antagonists. *Bioorg Med Chem Lett.* 2005; 15: 1333-1336.

14. Stebbins JL, Zhang Z, Chen J, Wu B, Emdadi A, Williams ME, Cashman J, Pellecchia M. Nuclear magnetic resonance fragment-based identification of novel FKBP12 inhibitors. *J Med Chem.* 2007; 50: 6607-6617.
15. Leffler M T, Volwiler EH. N-Aralkylmorpholines. *J Am Chem Soc.* 1938; 60: 896-899.
16. Khan SR, Bhanage BM. Selective hydroaminomethylation of olefins using simple and efficient Rh-phosphinite complex catalyst. *Appl Organometal Chem.* 2013; 27: 711-715.
17. Seth P, Ganapathy ME, Conway SJ, Bridges CD, Smith SB, Casellas P, Ganapathy V. Expression pattern of the type1 sigma receptor in the brain and identity of critical anionic amino acid residues in the ligand-binding domain of the receptor. *Biochim Biophys Acta* 2001; 1540: 59–67.
18. Kellogg GE, Abraham DJ. *Eur J Med Chem.* 2000; 35: 651-661.
19. Vilner BJ, Christy JS, Bowen WD. Sigma-1 and sigma-2 receptors are expressed in a wide variety of human and rodent tumor cell lines. *Cancer Res.* 1995; 55: 408-413.
20. Chu UB, Ruoho AE. Sigma receptor binding assays. [Curr Protoc Ele Pharmacol.](#) 2015; 71: 1.34.1-1.34.21.
21. Jones G, Willett P, Glen RC, Leach AR, Taylor R. Development and validation of a genetic algorithm for flexible docking. *J Mol Biol.* 1997; 267: 727-748.

## Graphical abstract

